Int. J. Solids Structures Vol. 22, No. 2, pp. 195–207, 1986
Printed in Great Britain.

0020–7683/86 $3.00 + .00

BIMATERIAL INTERFACE INSTABILITIES IN PLASTIC SOLIDS

PAUL S. STEIF
Department of Mechanical Engineering, Carnegie-Mellon University, Pittsburgh, PA 15213, U.S.A.

(*Received* 26 *October* 1984; *in revised form* 14 *March* 1985)

Abstract—A bifurcation analysis of a finite thickness layer embedded in an infinite body of different material properties is carried out. We investigate the conditions required for in-plane undulations confined to the vicinity of the bimaterial interface to develop from a state of homogeneous plane-strain tensile deformation. A deformation plasticity theory is employed, and the influence of the hardening rates and relative stiffness on the bifurcation strain is assessed. Particular attention is directed towards determining the effect of material properties on the competition between interface instabilities and localized shearing modes.

1. INTRODUCTION

The class of structural failure modes, which may be generically termed bifurcation phenomena, has received considerable attention in recent years. This class includes so-called geometric modes, such as buckling and necking, as well as "material instabilities" resulting in plastic-strain localization. Studies of these phenomena, however, have generally been confined to instances in which the material properties are spatially uniform. With the increasing interest in composite materials and their failure modes, it seems appropriate to examine how material heterogeneity can influence various bifurcation phenomena.

Biot, in his notable monograph[1], discusses a number of bifurcation problems, many involving bodies composed of different materials (piece-wise constant material properties). Particularly relevant to the present study is Biot's work on the buckling of a plate embedded in a medium of different properties. For the general orthotropic case he permits slip between the plate and the embedding medium, whereas perfect adherence is enforced when the materials are incrementally isotropic ("rubber-like"). Dorris and Nemat-Nasser[2] have considered the problem of a half space with a layer of differing properties at the free surface. The above studies were carried out for overall compressive loadings. Recently, Triantafyllidis and Maker[3] have treated the problem of an infinite periodically layered medium, with the goal of comparing microfailure and macrofailure modes under circumstances in which the equations governing the incremental deformation remain locally elliptic.

In this paper we focus on the deformation instabilities which can occur at a planar bimaterial interface in a body deformed in tension parallel to the interface, and on the competition between such instabilities and strain localization in either of the two materials. This study is motivated in part by the experimental observations of 100% pearlitic steels, which consist of pearlite colonies; each composed of alternating plates of ferrite and cementite. One finds that the metallurgical treatment which alters the absolute plate thicknesses (their ratio remaining roughly constant) also alters the microfailure mode, as well as macroscopic properties such as yield strength and ductility[4]. In particular, crack initiation in fine pearlites (smaller spacings) generally occurs via necking of the cementite plates, while strain localization in the ferrite is typically the crack precursor in coarse pearlites (larger spacings).

Here we investigate how the continuum deformation properties of the constituent layers influence interface instabilities (cementite necking) and shear band formation (in the ferrite and cementite). The specific problem to be addressed in this study is outlined in Section 2. We have reduced the number of independent parameters by one

(quite a few still remain) by taking one of the constituents to be semi-infinite in extent. (The ferrite–cementite thickness ratio is, approximately, seven to one.) It should be noted that in studying the interface instabilities here, we are in effect considering deformation modes which in a truly layered medium (finite thickness ratio) would have a period transverse to the layer interface which is identical with the layer periodicity. These are, in fact, the modes observed in a deforming pearlite colony. On the other hand, Triantafyllidis and Maker[3], in their search for the first microfailure mode in an infinite periodically layered structure, select from among a wider class of modes: most of which appear not to be relevant to pearlite.

2. DESCRIPTION OF PROBLEM

The geometry to be considered is shown in Fig. 1. A layer of width a is bounded above and below by perfectly bonded half spaces. The half spaces consist of one material labeled B, and the layer is another material labeled A. Deformations are confined to the (x_1, x_2) plane, and the materials are taken to be time independent and incompressible. Up to the current instant under consideration, the deformation has been a homogeneous straining, with the principal stretches along the x_1 and x_2 axes. Note that continuity of displacement at the interface is trivially satisfied. Both materials are assumed to be orthotropic along the x_1 and x_2 axes, with respect to incremental deformations from the current state. The study by Hill and Hutchinson[5] of bifurcation phenomena in a homogeneous rectangular block provides important background to bifurcation problems in general, and to the approach taken below in particular.

For incrementally linear solids, the material law is necessarily of the form (see [1])

$$\overset{\nabla}{\sigma}_{11} - \overset{\nabla}{\sigma}_{22} = 2\mu^*(\epsilon_{11} - \epsilon_{22}), \tag{1a}$$

$$\overset{\nabla}{\sigma}_{12} = 2\mu\epsilon_{12}, \tag{1b}$$

where $\overset{\nabla}{\sigma}_{ij}$ is the Jaumann derivative of the true stress, ϵ_{ij} is the Eulerian strain-rate, and subscripts refer to Cartesian components along the x_1 and x_2 axes. The incremental moduli μ and μ^* take on values μ_A and μ_A^* in A, and μ_B and μ_B^* in B. In an in-plane uniaxial tension test, $4\mu^*$ is the tangent modulus. In this constitutive law, the hydrostatic pressure increment has no influence on the deformation.

A solution to the boundary-value problem to be posed below is most easily arrived at via the nominal stress n_{ij}. In terms of the velocities v_i, the rates-of-change of n_{ij} are given by

$$\dot{n}_{11} - \dot{n}_{22} = [2\mu^* - \tfrac{1}{2}(\sigma_1 + \sigma_2)]\left(\frac{\partial v_1}{\partial x_1} - \frac{\partial v_2}{\partial x_2}\right), \tag{2a}$$

$$\dot{n}_{12} = [\mu + \tfrac{1}{2}(\sigma_1 - \sigma_2)]\frac{\partial v_2}{\partial x_1} + [\mu - \tfrac{1}{2}(\sigma_1 + \sigma_2)]\frac{\partial v_1}{\partial x_2}, \tag{2b}$$

$$\dot{n}_{21} = [\mu - \tfrac{1}{2}(\sigma_1 + \sigma_2)]\frac{\partial v_2}{\partial x_1} + [\mu - \tfrac{1}{2}(\sigma_1 - \sigma_2)]\frac{\partial v_1}{\partial x_2}, \tag{2c}$$

where σ_1 and σ_2 are the principal values of the Cauchy stress.

The incompressibility condition $(\partial v_1/\partial x_1) + (\partial v_2/\partial x_2) = 0$, implies the existence of a stream function $\psi(x_1, x_2)$ with

$$v_1 = \frac{\partial \psi}{\partial x_2}, \qquad v_2 = -\frac{\partial \psi}{\partial x_1}.$$

When ψ is inserted into the equations of incremental equilibrium

$$\dot{n}_{ij,i} = 0 \qquad \text{(summation over } i = 1, 2),$$

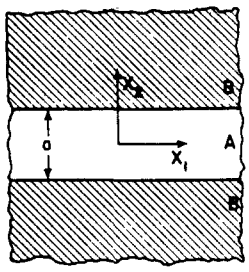

Fig. 1. Schematic representation of a finite layer embedded in a dissimilar material.

the following equation for ψ results:

$$(\mu + \tfrac{1}{2}\sigma)\frac{\partial^4\psi}{\partial x_1^2} + 2(2\mu^* - \mu)\frac{\partial^4\psi}{\partial x_1^2\partial x_2^2} + (\mu - \tfrac{1}{2}\sigma)\frac{\partial^4\psi}{\partial x_2^4} = 0. \tag{3}$$

In eqn (3) we have specialized to uniaxial plane-strain tension by taking $\sigma_1 = \sigma$ and $\sigma_2 = 0$. Equation (3) is taken to govern the incremental deformation in A and B with μ, μ^* and σ assuming their respective values in A and B.

Continuity of the incremental tractions and the velocities at the interface $x_2 = \pm(a/2)$ requires that

$$[\![\dot{n}_{22}]\!] = [\![\dot{n}_{21}]\!] = [\![v_1]\!] = [\![v_2]\!] = 0,$$

where $[\![\ ]\!]$ denotes the difference in the values of the enclosed quantity at the interface as one approaches from A and from B.

In terms of ψ, the continuity conditions are

$$\left[\!\left[(\mu - \tfrac{1}{2}\sigma)\left(\frac{\partial^2\psi}{\partial x_2^2} - \frac{\partial^2\psi}{\partial x_1^2}\right)\right]\!\right] = 0, \tag{4a}$$

$$\left[\!\left[(4\mu^* - \mu - \tfrac{1}{2}\sigma)\frac{\partial^3\psi}{\partial x_1^2\partial x_2} + (\mu - \tfrac{1}{2}\sigma)\frac{\partial^3\psi}{\partial x_2^3}\right]\!\right] = 0, \tag{4b}$$

$$\left[\!\left[\frac{\partial\psi}{\partial x_1}\right]\!\right] = \left[\!\left[\frac{\partial\psi}{\partial x_2}\right]\!\right] = 0. \tag{4c}$$

In eqn (4b), the continuity of $\dot{n}_{22,1}$ was used, which enabled the hydrostatic pressure increment to be eliminated.

The incremental equations are hyperbolic, parabolic or elliptic, according to whether there are four, two or zero real roots z to the equation

$$(\mu + \tfrac{1}{2}\sigma)z^4 + 2(2\mu^* - \mu)z^2 + (\mu - \tfrac{1}{2}\sigma) = 0.$$

Real roots z, signifying a loss of ellipticity, imply that localized shear deformations (shear bands) can emerge. Since the moduli and the stress are, in general, different in A and B, various combinations of regimes, e.g. hyperbolic in A and elliptic in B, are possible. To make the notation in the next section more concise, it is useful to introduce the quantities

$$R_A = \frac{\mu_A}{2\mu_A^*}, \quad S_A = \frac{\sigma_A}{4\mu_A^*}, \quad R_B = \frac{\mu_B}{2\mu_B^*}, \quad S_B = \frac{\sigma_B}{4\mu_B^*}, \quad \xi = \frac{\mu_B^*}{\mu_A^*}.$$

3. INTERFACE INSTABILITIES

At the current instant under consideration, a further increment in the far field displacements can, of course, give rise to a spatially uniform incremental deformation.

In this section we inquire as to whether spatially varying deformation patterns, consistent with the remotely imposed displacements, are also possible. In particular, we look for incremental deformations (eigenmodes), which are periodic in x_1, and which are confined to the vicinity of the interface. Such eigenmodes can be written in the form

$$\psi_A = f_A(x_2) \sin \frac{2\pi}{\lambda} x_1, \qquad \psi_B = f_B(x_2) \sin \frac{2\pi}{\lambda} x_1,$$

where λ is the wavelength of the deformation in the x_1 direction, and where $f_B(x_2)$ is such that $v_1(x_1, x_2) \to 0$ and $v_2(x_1, x_2) \to 0$ as $x_2 \to \pm\infty$. Attention is focused on modes which are symmetric about the x_1 axis, i.e.

$$v_1(x_1, x_2) = v_1(x_1, -x_2), \qquad v_2(x_1, x_2) = -v_2(x_1, -x_2).$$

Substituting the above forms for ψ_A and ψ_B into eqn (3) leads to a pair of homogeneous ordinary differential equations for f_A and f_B. Considering only $x_2 > 0$, the solutions $f(x_2)$ are linear combinations of

$$\sin \frac{2\pi}{\lambda} \alpha x_2, \qquad 0 < x_2 < \frac{a}{2},$$

in A, and

$$\exp\left[\frac{2\pi}{\lambda} \beta \left(x_2 - \frac{a}{2}\right)\right], \qquad x_2 > \frac{a}{2},$$

in B, where

$$\alpha^2 = \frac{R_A - 1 \pm \sqrt{S_A^2 - 2R_A + 1}}{R_A - S_A}$$

and

$$\beta^2 = \frac{1 - R_B \pm \sqrt{S_B^2 - 2R_B + 1}}{R_B - S_B}.$$

The root β must have negative real part, and the solutions for ψ_A and ψ_B must, of course, be real.

A description of the possible regimes for a single homogeneous material is given in [5] for the full range of values taken on by R and S. With two different materials, as in the present problem, there are many combinations of possible regimes. Instead of giving bifurcation conditions for all possible combinations, we will concentrate on the regimes most likely to be encountered with constitutive models typically used to describe metals.

The regimes of interest here are $R_A > S_A$, $R_A > 1$, together with $R_B > S_B$, $R_B > 1$. For $S_B < \sqrt{2R_B - 1}$, the equations in B are elliptic, and there are four complex conjugate roots β (two with negative real parts). For $S_B > \sqrt{2R_B - 1}$, the roots β are all pure imaginary, thus precluding instability modes which are confined to the vicinity of the interface. When $R_A > S_A > \sqrt{2R_A - 1}$, shear bands can emerge in A, and likewise for B when $R_B > S_B > \sqrt{2R_B - 1}$. The two cases considered below are for $S_A < \sqrt{2R_A - 1}$ and $R_A > S_A > \sqrt{2R_A - 1}$.

Case 1. $S_A < \sqrt{2R_A - 1}$

The equations are elliptic in A, and there are two pairs of complex conjugate roots α. The two linearly independent solutions for f_A may be written in the form

$$f_A = \mathrm{Re}\left\{c \sin \frac{2\pi}{\lambda} \alpha x_2\right\}, \tag{5}$$

where complex-valued c is the amplitude of the eigenmode, and Re{ } denotes the real part of the enclosed quantity. The first quadrant root $\alpha = p_A + ir_A$ is to be taken, where

$$p_A^2 + r_A^2 = \sqrt{\frac{R_A + S_A}{R_A - S_A}}, \qquad p_A^2 - r_A^2 = \frac{R_A - 1}{R_A - S_A}.$$

The linearly independent solutions for f_B are

$$f_B = \mathrm{Re}\left\{d \exp\left[\frac{2\pi}{\lambda} \beta \left(x_2 - \frac{a}{2}\right)\right]\right\}, \tag{6}$$

where complex-valued d is the amplitude of the eigenmode. The second-quadrant root $\beta = p_B + ir_B$ is to be taken ($p_B < 0$), where

$$p_B^2 + r_B^2 = \sqrt{\frac{R_B + S_B}{R_B - S_B}}, \qquad p_B^2 - r_B^2 = \frac{1 - R_B}{R_B - S_B}.$$

Substituting eqns (5) and (6) into continuity conditions (4), one obtains

$$(R_A - S_A)\,\mathrm{Re}\{c(1 - \alpha^2) \sin \alpha q\} = \xi(R_B - S_B)\,\mathrm{Re}\{d(\beta^2 + 1)\}, \tag{7a}$$

$$\mathrm{Re}\{c[(R_A - S_A)\alpha^2 - (R_A + S_A - 2)]\alpha \cos \alpha q\} = -\xi\,\mathrm{Re}\{d\beta[(R_B - S_B)\beta^2 + R_B + S_B - 2]\}, \tag{7b}$$

$$\mathrm{Re}\{c \sin \alpha q\} = \mathrm{Re}\{d\}, \tag{7c}$$

$$\mathrm{Re}\{c\alpha \cos \alpha q\} = \mathrm{Re}\{d\beta\}, \tag{7d}$$

where

$$q = \frac{\pi a}{\lambda}.$$

Interface instabilities are possible when the homogeneous set of equations (7) has a nontrivial solution. We now find an equation composed of real quantities, which expresses the vanishing of the determinant. With the relations

$$(R_A - S_A)(1 - \alpha^2) = \omega_A - i\theta_A, \quad (R_A - S_A)\alpha^2 - (R_A + S_A - 2) = \omega_A + i\theta_A,$$

$$(R_B - S_B)(1 + \beta^2) = \omega_B - i\theta_B, \quad (R_B - S_B)\beta^2 + (R_B + S_B - 2) = -\omega_B - i\theta_B,$$

where

$$\omega_A = 1 - S_A, \qquad \theta_A = \sqrt{2R_A - S_A^2 - 1},$$

$$\omega_B = 1 - S_B, \qquad \theta_B = \sqrt{2R_B - S_B^2 - 1},$$

one can use eqns (7c) and (7d) to eliminate d from eqns (7a) and (7b), yielding

$$\mathrm{Re}\left\{c\left[(\omega_A - i\theta_A)\sin\alpha q - \xi\left(\omega_B \sin\alpha q + \frac{\theta_B}{r_B}[p_B \sin\alpha q - \alpha\cos\alpha q]\right)\right]\right\} = 0,$$

$$\mathrm{Re}\left\{c\left[(\omega_A + i\theta_A)\alpha\cos\alpha q - \xi\left(\omega_B \alpha\cos\alpha q - \frac{\theta_B}{r_B}[X_B \sin\alpha q - p_B\alpha\cos\alpha q]\right)\right]\right\} = 0,$$

where

$$X_B = \sqrt{\frac{R_B + S_B}{R_B - S_B}}.$$

Now, since $\mathrm{Re}\{cu\} = 0$ and $\mathrm{Re}\{cv\} = 0$ together imply that $\mathrm{Im}\{\bar{u}v\} = 0$ (imaginary part of $\bar{u}v$), one can, after some lengthy but straightforward manipulation, deduce the bifurcation equation

$$\begin{aligned}
&\frac{1}{2r_A}\sinh 2r_A q\left\{(1 - S_A)X_A + S_A - \xi[(R_B - S_B)(1 - X_B)(X_A - 1)]\right.\\
&\quad\left. + \xi^2\frac{(R_B - S_B)}{(R_A - S_A)}[(1 - S_B)X_B + S_B]\right\} + \frac{1}{2p_A}\sin 2p_A q\left\{(1 - S_A)X_A - S_A\right.\\
&\quad\left. - \xi[(R_B - S_B)(1 - X_B)(X_A + 1)] - \xi^2\frac{(R_B - S_B)}{(R_A - S_A)}[(1 - S_B)X_B + S_B)]\right\}\\
&\quad - \xi(R_B - S_B)p_B\{X_A[\cosh 2r_A q + \cos 2p_A q] + X_B[\cosh 2r_A q - \cos 2p_A q]\} = 0,
\end{aligned} \tag{8}$$

where

$$X_A = \sqrt{\frac{R_A + S_A}{R_A - S_A}}.$$

One interesting special case of eqn (8) is when the wavelength becomes arbitrarily short, i.e. $q \to \infty$. In this limit, the bifurcation equation becomes

$$\begin{aligned}
&\frac{1}{R_B - S_B}[(1 - S_A)X_A + S_A] + \xi^2\frac{1}{R_A - S_A}[(1 - S_B)X_B + S_B]\\
&\qquad - \xi[X_A + X_B - X_A X_B - 1 + 2r_A p_B(X_A + X_B)] = 0.
\end{aligned} \tag{9}$$

This bifurcation corresponds to an interface instability between two half spaces, the length scale of the instability being immaterial to the bifurcation condition. An inspection of eqn (9) reveals that it is symmetric in the A and B quantities, as it should be.

We note that as $\xi \to 0$, the bifurcation eqn (8) reduces to the symmetric elliptic regime bifurcation condition for a homogeneous rectangular block, characterized by S_A and R_A, as given by eqn (5.11) in [5]. In the limit as $\xi \to \infty$, the problem reduces to the free-surface instability of a half space, characterized by S_B and R_B, which has been studied by Hutchinson and Tvergaard[6]. In fact, eqn (8) reduces to eqn (2.16) in [6] (or eqn (6.5) in [5]) in that limit.

Case 2. $\sqrt{2R_A - 1} < S_A < R_A$

The equations are hyperbolic in A, and there are four real roots α. The solution for f_A is of the form

$$f_A = c_1 \sin \frac{2\pi}{\lambda} p_A x_2 + c_2 \sin \frac{2\pi}{\lambda} r_A x_2, \tag{10}$$

where p_A and r_A may be taken positive, and are given by

$$p_A^2 = \frac{R_A - 1 + \sqrt{S_A^2 - 2R_A + 1}}{R_A - S_A}, \qquad r_A^2 = \frac{R_A - 1 - \sqrt{S_A^2 - 2R_A + 1}}{R_A - S_A}.$$

The solution for f_B remains the same as when $S_A < \sqrt{2R_A - 1}$.

Continuity conditions (7) now become

$$c_1(\omega_A - \theta_A) \sin p_A q + c_2(\omega_A + \theta_A) \sin r_A q = \xi(R_B - S_B) \operatorname{Re}\{d[\beta^2 + 1]\}, \tag{11a}$$

$$c_1(\omega_A + \theta_A) p_A \cos p_A q + c_2(\omega_A - \theta_A) r_A \cos r_A q = -\xi \operatorname{Re}\{d\beta[(R_B - S_B)\beta^2 + R_B + S_B - 2]\}, \tag{11b}$$

$$c_1 \sin p_A q + c_2 \sin r_A q = \operatorname{Re}[d], \tag{11c}$$

$$c_1 p_A \cos p_A q + c_2 r_A \cos r_A q = \operatorname{Re}[d\beta], \tag{11d}$$

where ω_A, ω_B and θ_B are the same as above, but now $\theta_A = \sqrt{S_A^2 - 2R_A + 1}$.

One can eliminate d as was done above and eventually obtain the bifurcation equation

$$\begin{aligned}(R_A - S_A)^2[(1 - p_A^2)^2 Q_p W_r - (1 - r_A^2)^2 Q_r W_p] - 2\xi(R_B - S_B)(R_A - S_A) \\ \times \{(1 - X_B)[(1 - p_A^2)Q_p W_r - (1 - r_A^2)Q_r W_p] - p_B(p_A^2 - r_A^2)[X_B Q_p Q_r \\ + W_r W_p]\} + 2(R_B - S_B)\xi^2[(S_B - 1)X_B - S_B][Q_p W_r - Q_r W_p] = 0,\end{aligned} \tag{12}$$

where

$$Q_p = \sin p_A q, \qquad Q_r = \sin r_A q, \qquad W_p = p_A \cos p_A q, \qquad W_r = r_A \cos r_A q.$$

Taking the limit as $\xi \to 0$ in eqn (12), one recovers eqn (5.13) in [5], the symmetric bifurcation of a rectangular block in the hyperbolic regime. Again, with hyperbolic equations governing the deformation in A, a localized shearing mode in A is also possible.

4. NUMERICAL RESULTS AND DISCUSSION

In this section numerical results are presented for a particular constitutive model. The particular choice of constitutive model reflects the accumulating evidence in recent years that theoretical predictions of bifurcation phenomena depend sensitively on the precise constitutive model employed. In particular, bifurcation strains tend to be overestimated when one uses flow theories based on a smooth yield surface. Plasticity theories which permit a more compliant response to nonproportional stress increments, for example, models which allow a vertex to develop at the loading point of the yield surface, lead to more realistic estimates of bifurcation strains. One may represent the moduli for the total loading regime at a yield-surface vertex by the moduli derived from a deformation theory of plasticity. This approach was employed by Hutchinson and Tvergaard[6] in their study of free-surface instabilities.

Consequently, we choose to confine ourselves to a single constitutive model which permits a realistic response to nonproportional stress increments, and to examine the effect of varying stiffnesses and hardening rates. Materials A and B are modeled by a finite-strain-deformation theory (nonlinear hyperelastic solid), with a uniaxial true stress–logarithmic strain relation of the form

$$\sigma = k\epsilon^N,$$

where the hardening rate N and the stiffness parameter k are, in general, different in materials A and B. When specialized to plane-strain tension, the parameters relevant to the bifurcation analysis are found to be

$$\frac{\sigma}{4\mu^*} = \frac{\epsilon}{N}, \qquad \frac{\mu}{2\mu^*} = \frac{\epsilon}{N}\coth(2\epsilon), \qquad \frac{\mu_B^*}{\mu_A^*} = \frac{k_B}{k_A}\frac{N_B}{N_A}\epsilon^{(N_B - N_A)}.$$

Thus R and S depend only on N, whereas ξ depends on the relative stiffness $k_r \equiv k_B/k_A$, as well as on the hardening rates. With a view towards exploring the range of parameters which appears to be relevant to pearlite, we concentrate on relatively low hardening rates N_A.

In what follows, the cases of $q \to \infty$ and q remaining finite are considered separately. For $q \to \infty$, the interface instability is occurring between two half spaces, and the bifurcation equation (9) governs the instability. Since materials A and B are on an equal footing, one can, without loss of generality, consider k_r to be less than 1, i.e. that A is stiffer.

In Figs. 2 and 3, the hardening rate in A has been fixed at $N_A = 0.025$ and $N_A = 0.1$, respectively; the solid curves show the bifurcation strain ϵ^*, as calculated from eqn (9), as a function of the relative stiffness k_r for a variety of hardening rates N_B. For $N_A = 0.025$, the free-surface instability occurs at $\epsilon = 0.118$, and for $N_A = 0.1$ at $\epsilon = 0.252$. It is readily seen that the interface instability always occurs at a strain which is larger than the strain at which the stiffer material exhibits a free-surface instability.

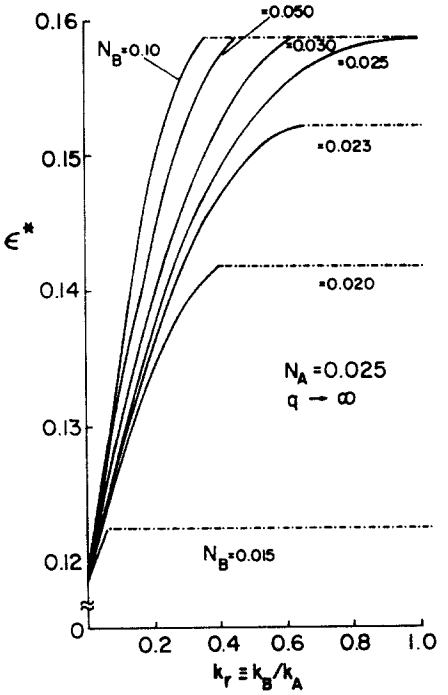

Fig. 2. Bifurcation strain for two bonded half spaces, as a function of relative stiffness k_r; the stiffer half space having a hardening rate $N_A = 0.025$. (—— ~ A and B in elliptic regime; –·–·– ~ A or B enters hyperbolic regime.)

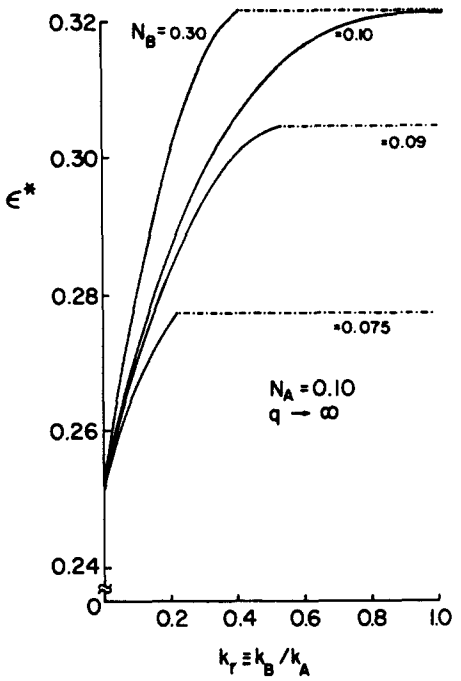

Fig. 3. Bifurcation strain for two bonded half spaces, as a function of relative stiffness k_r; the stiffer half space having a hardening rate $N_A = 0.10$. (—— ~ A and B in elliptic regime; –·–·– ~ A or B enters hyperbolic regime.)

Also, variations in ϵ^* are more sensitive to changes in k_r than to changes in N_B. The hardening rate N_B is very influential, however, in determining the range of k_r in which interface instability precedes the appearance of shear bands. The dash–dot curves in Figs. 2 and 3 indicate the value of strain at which material A or B enters the hyperbolic regime, thus signifying the emergence of shear bands. This also corresponds to the root α or β becoming pure imaginary, with the instability no longer confined to the vicinity of the interface.

We first note that the more disparate the stiffnesses, i.e. the smaller k_r, the greater the likelihood of an interface instability preceding shear bands. Let k_r^* be such that when $k_r > k_r^*$, shear bands are the first bifurcation mode. For $N_B < N_A$, the quantity k_r^* increases with N_B, until $N_B = N_A$ at which point $k_r^* = 1$. When $N_A = N_B$ and $k_r = 1$, bifurcation occurs just as the homogeneous material enters the hyperbolic regime. In addition to the shear banding, the material also exhibits an instability, no longer confined to the interface, which is the tensile analog of Biot's "internal buckling."

For N_B increasing above N_A, k_r^* decreases, and now shear bands appear in A when $k_r > k_r^*$. Although they are not shown in Figs. 2 and 3, the bifurcation curves for very high hardening rates, for example $N_B = 0.7$ and 0.9, shift somewhat to the right; that is k_r^* increases again. This range of hardening is generally not observed in metals.

Returning to $N_B < N_A$, one finds that for N_B sufficiently small k_r^* approaches 0. This corresponds to the case in which material A first develops a free-surface instability at a strain at which material B has already entered the hyperbolic regime. Such a combination of N_A and N_B always exhibits shear bands as its first bifurcation mode, regardless of the relative stiffness ($0 < k_r < 1$). In Fig. 4 we have plotted, as a function of N_A, the value N_B^*, below which no interface instability is possible. This curve is described parametrically by

$$\epsilon[1 - e^{-2\epsilon}] = N_A, \qquad \frac{2\epsilon}{N_B^*} \coth 2\epsilon - \left(\frac{\epsilon}{N_B^*}\right)^2 = 1.$$

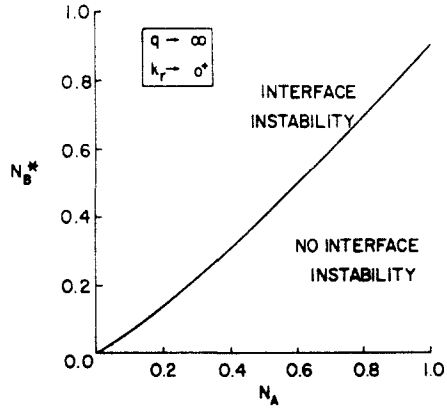

Fig. 4. Dependence of minimum hardening rate N_B^* for interface instability on hardening rate N_A of stiffer half space.

Cases in which q remains finite are depicted in Figs. 5–7. In an actual layered structure, one may be interested in what occurs as $q \to 0$, i.e. when the wavelength becomes long compared with the layer thicknesses. Unfortunately, because we have taken one of the layers, namely B, to be semi-infinite in extent, the wavelength can never be long compared with layer B. In fact, as was noted by Dorris and Nemat-Nasser[2], who had the same difficulty with one of the media being semi-infinite, no interface instability occurs for $q \to 0$.

Recall, however, that if $\xi \to 0$ or ∞ in eqn (8), the various homogeneous medium bifurcations are recovered, including the bifurcation as $q \to 0$. In fact, the limits as $q \to 0$ and $\xi \to 0$, or $q \to 0$ and $\xi \to \infty$, are nonuniform. The result of Hill and Hutchinson[5], is recovered if $\xi \to 0$ faster than $q \to 0$, in the sense that

$$\xi \sim o(q) \qquad \text{as} \quad q \to 0.$$

For the free-surface instability of a half space[6] to be recovered, the relative magni-

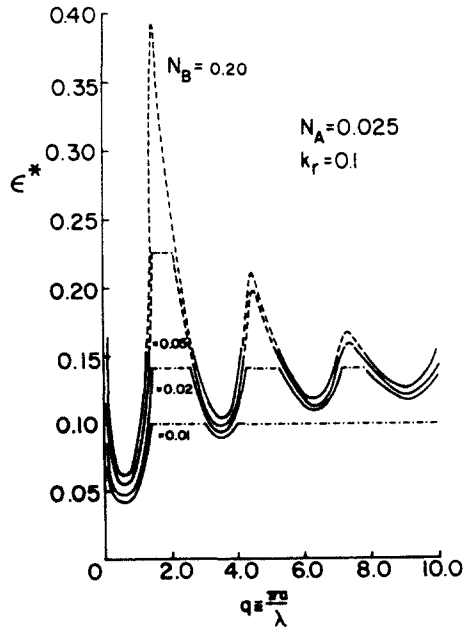

Fig. 5. Variation of bifurcation strain ϵ^* with dimensionless wave number q for several values of hardening rate N_B, with $N_A = 0.025$ and $k_r = 0.1$. (—— ~ A and B in elliptic regime; – – – – ~ A in hyperbolic regime, B in elliptic regime; –·–·– ~ B enters hyperbolic regime.)

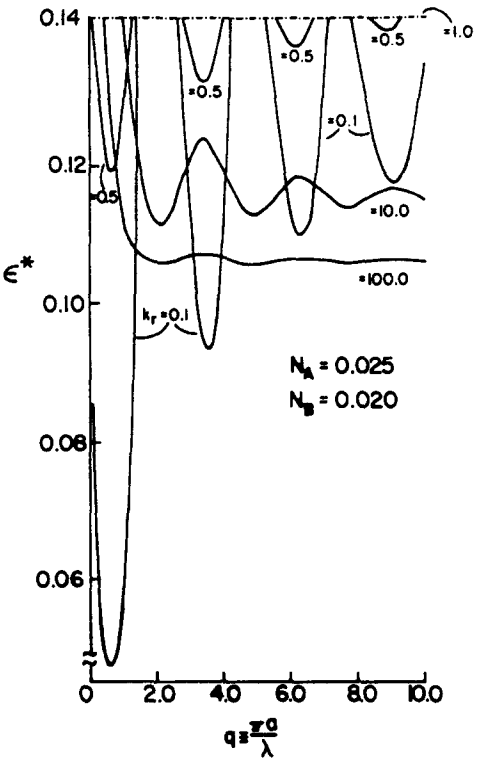

Fig. 6. Variation of bifurcation strain ϵ^* with dimensionless wave number q for several values of relative stiffness k_r, with $N_A = 0.025$ and $N_B = 0.020$. (—— ~ A and B in elliptic regime; -·-·- ~ B enters hyperbolic regime).

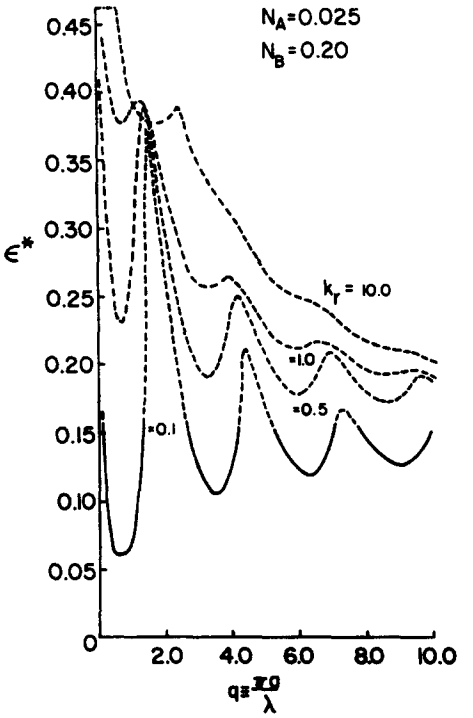

Fig. 7. Variation of bifurcation strain ϵ^* with dimensionless wave number q for several values of relative stiffness k_r, with $N_A = 0.025$ and $N_B = 0.20$. (—— ~ A and B in elliptic regime; - - - - ~ A in hyperbolic regime, B in elliptic regime; -·-·- ~ B enters hyperbolic regime).

tudes of ξ and q must be such that

$$\frac{1}{\xi} \sim o(q^3) \qquad \text{as} \quad q \to 0.$$

Thus for a given small value of q, recovering the half space, free-surface instability requires far more disparate stiffnesses than recovering the rectangular block bifurcation.

In Figs. 5–7, the bifurcation strain ϵ^* is plotted against q. In these figures, three types of bifurcation are distinguished: (i) interface instability with both A and B in the elliptic regime (solid lines); (ii) interface instability with A hyperbolic and B elliptic (dashed lines); (iii) B turns hyperbolic, and hence an instability confined to the interface is impossible, and shear bands can emerge in B (dash–dot lines). Of course when A turns hyperbolic, shear bands may emerge in A, in addition to any possible interface instability.

Consider a low hardening layer between half spaces of less stiff material. This case is shown in Fig. 5, in which we have set $N_A = 0.025$ and $k_r = 0.1$, and have examined the effect of varying N_B. Generally, for a fixed value of q, the change in ϵ^* with a change in N_B is relatively modest, provided an interface instability is still possible. The change in ϵ^* is somewhat more substantial when q takes on values near to those at which a finite homogeneous block of A would have its first symmetric bifurcation in the hyperbolic regime. As was the case for $q \to \infty$, the major effect of N_B is to alter significantly the range of parameters over which an interface instability can occur. In fact, for $N_B = 0.01$, an interface instability is possible only for a very limited range of q. Note that for $N_B = 0.01$ no interface instability is possible as $q \to \infty$. As N_B increases, the ranges of q over which interface instabilities are possible expand; for $N_B = 0.2$, interface instabilities occur over the entire range of q, except in a small neighborhood about $q = 0$.

In Fig. 6, the bifurcation strain ϵ^* is plotted against the dimensionless wave number q for a range of values of k_r. We have held the hardening rates fixed at $N_A = 0.025$ and $N_B = 0.020$, two relatively nondisparate values. Since $N_A > N_B$, an interface instability with A hyperbolic is not possible; thus there are no dashed curves. For this pair of hardening rates, one can span the range from the finite-block bifurcation to the half space free-surface instability by varying k_r from 0 to ∞. The curve for $k_r = 0.1$ is very close to the curve for the finite-block bifurcation, except for $q < 0.6$ and near the maxima at which shear bands in B intervene. For $k_r \to \infty$, the solution to eqn (8) approaches $\epsilon^* = 0.105$, the free-surface instability strain for $N = 0.020$, independent of wavelength. This approach can be seen in the curves labeled $k_r = 10.0$ and $k_r = 100.0$. The variations in ϵ^* with q diminish progressively, and the value of q, below which shear bands intervene, also decreases with increasing k_r. When $k_r = 1.0$, not only are shear bands the first bifurcation mode as $q \to \infty$ (as seen in Fig. 2), but for all finite values of q as well. As will be seen below, this need not be so if the hardening rates are very different.

Figure 7 depicts a case in which the hardening rates are more disparate: $N_A = 0.025$ and $N_B = 0.2$. Now, with $k_r \ll 1.0$, the rectangular-block bifurcation is recovered over the entire range of q (except near $q = 0$); material B goes hyperbolic at a strain which exceeds the bifurcation strain of the rectangular block. As k_r increases, the results appear very different than those shown in Fig. 6. First, if we take k_r larger than some value (between 0.1 and 0.5), an interface instability cannot occur while A is elliptic. Second, for $k_r = 10.0$, the free-surface instability for $N = 0.2$, which would occur at $\epsilon^* = 0.377$, is not recovered. When k_r was increased to $k_r = 200.0$, a mode similar to a free-surface instability was observed in the range $1.0 < q < 3.0$. As q was increased above 3.0, the bifurcation strain diminished steadily towards $\epsilon^* = 0.118$: the elliptic–hyperbolic transition point in A.

This result ought not to be surprising in that no interface instability is possible for q and k both approaching ∞ (see Fig. 4). A closer examination of the bifurcation equation

(12) reveals that, for $\xi \to \infty$, bifurcation can occur if

$$r_A \sin p_A q \cos r_A q - p_A \sin r_A q \cos p_A q = 0, \tag{13}$$

as well as if the free-surface bifurcation condition

$$(S_B - 1)X_B - S_B = 0$$

is satisfied. One solution to eqn (13) is $p_A = r_A$, which is precisely satisfied at the elliptic–hyperbolic transition. In fact, there is always a solution to eqns (11) at the elliptic–hyperbolic transition point of material A; at that point $p_A = r_A$, $\theta_A = 0$, $d = 0$ and $c_1 = -c_2$. This bifurcation corresponds to no incremental displacement at the interface, and is analogous to Biot's "internal buckling" of a plate which is cemented between two rigid half spaces. For q exceeding 3.0, the decreasing bifurcation strain involves the increasing importance of the terms

$$r_A \sin p_A q \cos r_A q - p_A \sin r_A q \cos p_A q$$

in eqn (12). Since this mode involves no disturbance of the interface, it is not clear that it would play a role in the microfailure of a layered structure.

5. CONCLUSIONS

This study has shown that one can understand qualitatively the effect of material properties on the competition between modes by examining the case in which the interface instability occurs between half spaces. The relative stiffness of the two materials influences the strain at which undulations appear, as well as whether undulations develop at all prior to shear banding. Hardening rates tend principally to influence the competition between modes. Generally, similar hardening rates and dissimilar stiffnesses lead to undulations preceding shear bands. A resolution of what precisely occurs when the wavelength of the interface instability is very long awaits consideration of the finite-thickness ratio problem, though such modes appear not to be relevant to the deformation of pearlite.

Acknowledgement—This work has been supported by the Association of American Railroads through the Affiliated Laboratory at Carnegie-Mellon University.

REFERENCES

1. M. A. Biot, *Mechanics of Incremental Deformation*. Wiley, New York (1965).
2. J. F. Dorris and S. Nemat-Nasser, *J. Appl. Mech.* **47**, 304 (1980).
3. N. Triantafyllidis and B. N. Maker, On the comparison between microscopic and macroscopic instability mechanisms in a class of fiber reinforced composites. *J. Appl. Mech.* (to appear).
4. D. J. Alexander and I. M. Bernstein, *Phase Transformations in Ferrous Alloys* (Edited by A. R. Marder and J. Goldstein), pp. 243–257 TMS, Warrendale, Pennsylvania (1984) (to be published).
5. R. Hill and J. W. Hutchinson, *J. Mech. Phys. Solids* **23**, 239 (1975).
6. J. W. Hutchinson and V. Tvergaard, *Int. J. Mech. Sci.* **22**, 339 (1980).